Gfi1b: a key player in the genesis and maintenance of acute myeloid leukemia and myelodysplastic syndrome

Aniththa Thivakaran,[1] Lacramioara Botezatu,[1] Judith M. Hönes,[1,2] Judith Schütte,[1] Lothar Vassen,[1] Yahya S. Al-Matary,[1] Pradeep Patnana,[1] Amos Zeller,[1] Michael Heuser,[3] Felicitas Thol,[3] Razif Gabdoulline,[3] Nadine Olberding,[1] Daria Frank,[1] Marina Suslo,[1] Renata Köster,[1] Klaus Lennartz,[4] Andre Görgens,[5,6] Bernd Giebel,[5] Bertram Opalka,[1] Ulrich Dührsen[1] and Cyrus Khandanpour[1,7]

[1]Department of Haematology, West German Cancer Center, University Hospital Essen, University of Duisburg-Essen, Essen, Germany; [2]Department of Endocrinology, Diabetes and Metabolism, University Hospital Essen, University of Duisburg-Essen, Essen, Germany; [3]Department of Haematology, Haemostaseology, Oncology, and Stem Cell Transplantation, Medical University of Hannover, Germany; [4]Institute for Cell Biology, University Hospital Essen, University of Duisburg-Essen, Essen, Germany; [5]Institute for Transfusion Medicine, University Hospital Essen, University of Duisburg-Essen, Essen, Germany; [6]Department of Laboratory Medicine, Karolinska Institutet, Stockholm, Sweden and [7]Department of Medicine A, Hematology, Oncology and Pneumology, University Hospital Münster, Germany

 doi:10.3324/haematol.2017.167288

Received: June 29, 2017.

Accepted: January 5, 2018.

Pre-published: January 11, 2018.

Correspondence: cyrus.khandanpour@uk-essen.de

Supplementary Information

Boundaries of *GFI1B* expression

We grouped patients based on *GFI1B* expression and found a correlation between *GFI1B* expression and a similar gene signature as well as survival with the following boundaries: Boundaries defined as 0%-15% of maximum observed *GFI1B* expression (low) and 16%-100% (100% was set as the highest observed *GFI1B*-expression) of *GFI1B* expression for AML patients predicted the outcome of patients. We selected different boundaries for *GFI1B* expression level and correlated these boundaries with the outcome of patients regarding event free survival and overall-survival. At a setting of 15%, meaning that the outcome of patients with the 15% lowest expression level of *GFI1B* were compared to the patients with expression level of *GFI1B* higher than 15%, the difference in event free survival and overall survival was different and enough patients were included in both group to reach significance. We normalized the gene expression arrays of the MDS patient to the values for the AML expression and set similar boundaries. However, with regard to the *GFI1B* expression level observed in the MDS cohort, low expression corresponded to 0%-30% of the maximum observed *GFI1B* expression level in the MDS cohort and high expression to 31%-100% of the highest observed *GFI1B* expression level in the MDS cohort.

Gene expression analysis and pathway analysis of available human and mouse *GFI1B/Gfi1b* data sets

CEL files of microarray data of AML samples from GSE6891 and GSE1159 were processed using AltAnalyze (http://www.altanalyze.org/) [1]. Standard analysis parameters were not changed. Samples were then sorted for *GFI1B* expression (20% of highest expressing samples versus 5% of lowest expressing samples) and GO-ELITE analysis was done using AltAnalyze and standard parameters again, the minimum fold change was set to 1.5.

To identify pathways that were activated in *GFI1B* high samples compared to *GFI1B* low samples we employed (S)ignaling (P)athway (E)nrichment using (E)xperimental (D)atasets SPEED analysis (http://speed.sys-bio.net) [2, 3]. The SPEED enrichment algorithm extracts signature gene sets per pathway from microarray experiments and compares an input gene list against the signature genes using Fisher's exact test. The reported p-value is a one-tailed calculation. Multiple hypothesis correction is achieved by calculating a false discovery rate described in [4].The top 500 upregulated and 500 downregulated probe sets from GEO AML dataset GSE6891 were annotated with their official gene symbols, duplicates were removed and the resulting 618 unique gene symbols were subjected to analysis using standard parameters and additional selection of H_2O_2 and MAPK. The results are shown as a table.

Analysis of leukemic mice

Moribund mice were analysed by staining BM and spleen cells with the following fluorochrome-conjugated antibodies: CD11b, Gr-1, B220, Ter119, CD8a, CD4, CD117 (c-kit) and Annexin (Biolegend). Measurements were performed using LSR II or FLOWScan flow cytometers (BD Biosciences). To measure the intracellular ROS level, BM cells from leukaemic mice were first stained with CD117 (c-Kit) (Biolegend). After washing with DPBS (Gibco), the ROS level was analysed using a DCFDA Cellular ROS Detection Assay Kit (Abcam), according to the manufacturer's instructions. The measurements were performed using an LSR II flow cytometer (BD Biosciences). For phosphorylated p38 MAP kinase and phosphorylated Akt intracellular staining, BM were stained for cell surface markers, and the cells were treated with fixation buffer and Perm buffer III, purchased from (BD Biosciences), and stained with anti-phospho-p38 ($pThr^{180}/pY^{182}$) and anti-phospho-Akt (pS473) antibodies (BD Biosciences).

Western Blot

Nuclear and cytoplasmic extractions were performed with NE-PER Nuclear and Cytoplasmic Extraction Reagents (Thermo Scientific).

Antibodies used for Western blotting included Gfi1b (D-19, sc-8559x, Santa Cruz Biotechnology), donkey anti-goat IgG-HRP (sc-2020, Santa Cruz Biotechnology), Lamin B(C-20) (sc-6216, Santa Cruz Biotechnology) and FoXO3 (75D8) rabbit mAb (#2497, Cell Signalling).

Polymerase chain reaction (PCR) genotyping

To confirm efficient excision of the *Gfi1b* allele after poly (I:C) treatment, PCR genotyping using leukaemic BM cells derived from *Gfi1b*$^{fl/fl}$*MxCre*^{tg}*NUP98/HOXD13* mice was performed using primers from a previous publication.[5] The product length of the floxed allele is 295 and 540 for the deleted allele.

DNA- Microarray

For microarray analyses, we used the Affymetrix GeneChip platform employing the Express Kit protocol for sample preparation and microarray hybridization. Total RNA (200 ng) was converted into biotinylated cRNA, purified, fragmented and hybridized MG-430_2.0 microarrays (Affymetrix). The arrays were washed and stained according to the manufacturer's recommendation and finally scanned in a GeneChip scanner 3000 (Affymetrix) with G7 update. Signal summarization (RMA algorithm) and statistical analysis by ANOVA was performed with PartekGS. Data are available at http://www.ncbi.nlm.nih.gov/geo/query/acc.cgi?acc=GSE88882.

ChIP-Seq analysis and DNA–microarray analysis data are available as a super series at http://www.ncbi.nlm.nih.gov/geo/query/acc.cgi?acc=GSE88935.

GSEA analysis

For gene set enrichment analysis expression data generated by AltAnalyze was analyzed using GSEA software (http://software.broadinstitute.org/gsea/index.jsp) [6, 7].

The standard analysis parameters were not changed except the number of plot-graphs for the top set of phenotypes was set to 60. The data were analyzed by GSEA based on complete probeset results.

CEL files of microarray data from Gfi1b wt and ko mice were processed using Affymetrix™ Expression Console 1.4.1 and mta-gene-full parameters followed by Affymetrix Transcriptome Analysis Console 3.1 (TAC) analysis using standard parameters or dataset analysis using AltAnalyze and GSEA as described above.

Statistical methods

Student's t-test was performed to determine significantly different percentage values. For other statistical analyses, either paired or unpaired analysis was used. An analysis of the survival of different murine cohorts was performed using the Gehan-Breslow-Wilcoxon test. All *p* values reported are two-sided and considered significant at ≤0.05. All analyses were performed using GraphPad Prism 5 or 6 software (GraphPad Software, La Jolla, CA, USA) or SSP version 19 (IBM).

Supplementary Figure 1 Thivakaran et al.

A

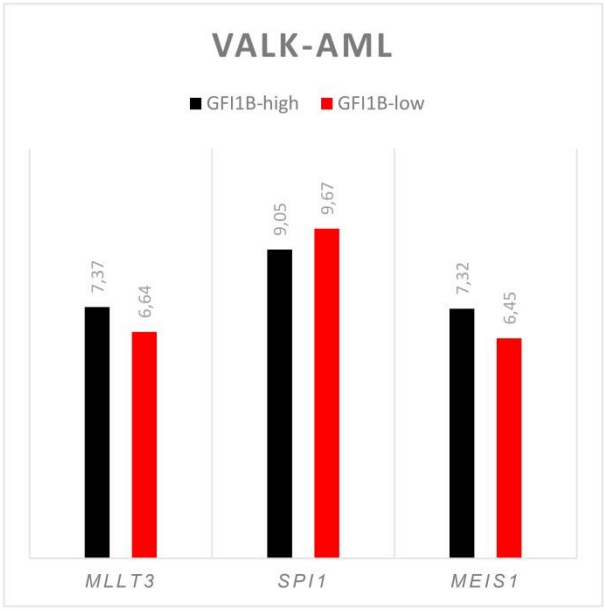

Supplementary Figure 1

A. Gene expression of *MLLT3*, *SPI1* and *MEIS1* in *GFI1B*-high and *GFI1B*-low human Valk-AML data set.

Supplementary Figure 2 Thivakaran et al.

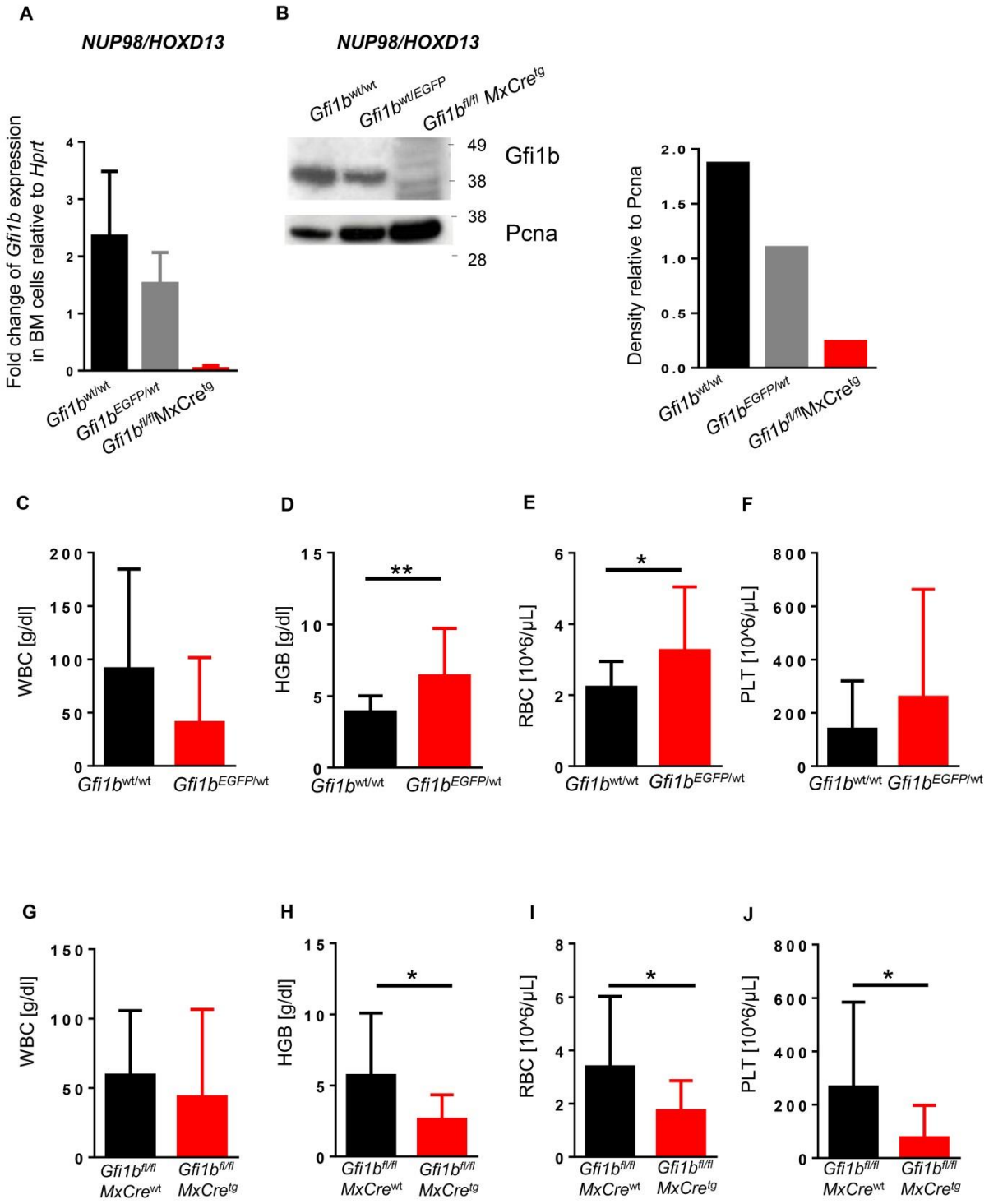

Supplementary Figure 2

A. Fold change in *Gfi1b* gene expression at the mRNA level in BM cells derived from *Gfi1b*$^{wt/wt}$ (n=5), *Gfi1b*$^{EGFP/wt}$ (n=5) and *Gfi1b*$^{fl/fl}$ *x MxCre*^{tg} *NUP98/HOXD13*^{tg} mice (n=3).

B. Western blot for Gfi1b of nuclear extracts of *Gfi1b*$^{wt/wt}$, *Gfi1b*$^{EGFP/wt}$ and *Gfi1b*$^{fl/fl}$*MxCre*^{tg}*NUP98/HOXD13*^{tg} mice. PCNA was used as a loading control. Numbers indicate size in kDa. The density plot was analysed relative to the *PCNA* expression.

C. Median values for white blood cell (WBC) count of *Gfi1b*$^{wt/wt}$ (n=15) and *Gfi1b*$^{EGFP/wt}$*NUP98/HOXD13*^{tg} (n=15) leukaemic mice.

D. Median values for haemoglobin (HGB) of *Gfi1b*$^{wt/wt}$ (n=15) and *Gfi1b*$^{EGFP/wt}$*NUP98/HOXD13*^{tg} (n=16) leukaemic mice, **p=0.0090.

E. Median values for red blood cell (RBC) number of *Gfi1b*$^{wt/wt}$ (n=15) and *Gfi1b*$^{EGFP/wt}$*NUP98/HOXD13*^{tg} (n=16) leukaemic mice, *p=0.0473.

F. Median values for platelet (PLT) number of *Gfi1b*$^{wt/wt}$ (n=-15) and *Gfi1b*$^{EGFP/wt}$*NUP98/HOXD13*^{tg} (n=16) leukaemic mice.

G. Median values for white blood cell (WBC) count of *Gfi1b*$^{fl/fl}$*MxCre*^{wt} (n=13) and *Gfi1b*$^{fl/fl}$*MxCre*^{tg}*NUP98/HOXD13*^{tg} (n=14) leukaemic mice.

H. Median values for haemoglobin (HGB) of *Gfi1b*$^{fl/fl}$*MxCre*^{wt} (n=13) and *Gfi1b*$^{fl/fl}$*MxCre*^{tg}*NUP98/HOXD13*^{tg} (n=14) leukaemic mice, *p=0.0224.

I. Median values for red blood cell (RBC) number of *Gfi1b*$^{fl/fl}$*MxCre*^{wt} (n=13) and *Gfi1b*$^{fl/fl}$*MxCre*^{tg}*NUP98/HOXD13*^{tg} (n=14) leukaemic mice, *p=0.0434.

J. Median values for platelet number (PLT) of *Gfi1b*$^{fl/fl}$*MxCre*^{wt} (n=13) and *Gfi1b*$^{fl/fl}$*MxCre*^{tg}*NUP98/HOXD13*^{tg} (n=14) leukaemic mice, *p=0.0465.

Supplementary Figure 3 Thivakaran et al.

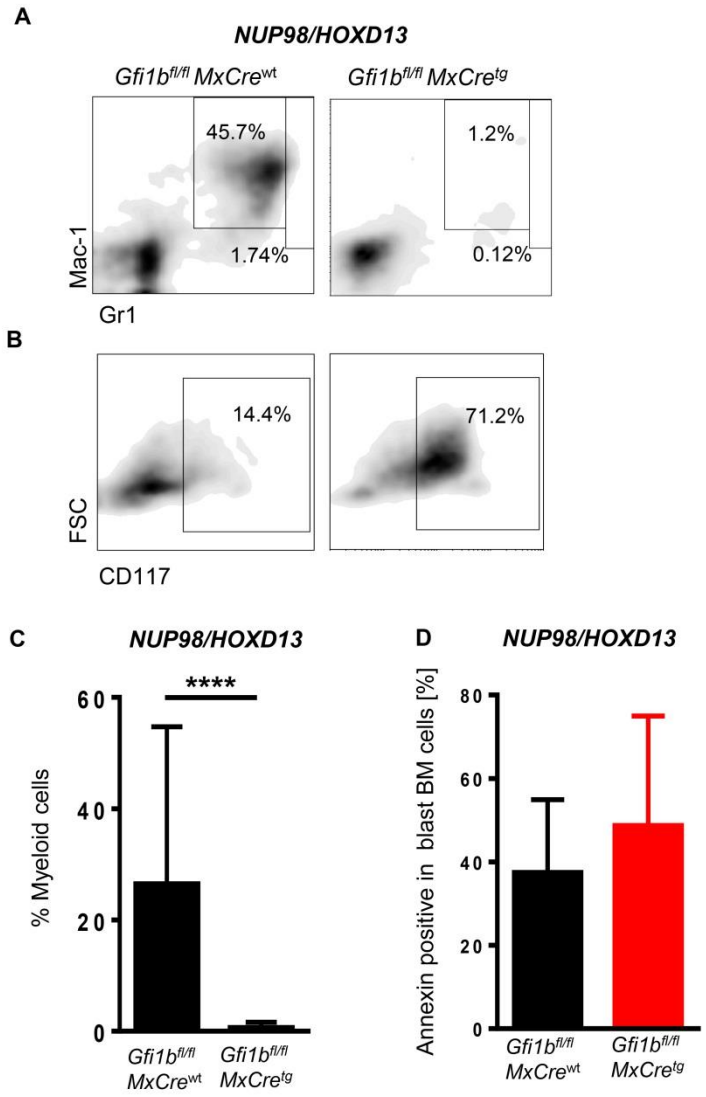

Supplementary Figure 3

A. The frequency of macrophages (Mac-1^{hi}Gr-1^{int}) (left panel, ****p<0.0001) and granulocytes (Mac-1^{hi}Gr-1^{hi}) (right panel, *p=0.0206) in the BM of the mice described in Figure 3F, (n=15 for *Gfi1b*$^{fl/fl}$*MxCre*^{wt} mice and n=14 for *Gfi1b*$^{fl/fl}$*MxCre*^{tg}*NUP98/HOXD13*^{tg} mice).

B. The frequency of $CD117^{+}$ (also known as c-Kit^{+}) cells in the BM of the mice described in Figure 3F, (****p<0.0001), n=15 for *Gfi1b*$^{fl/fl}$*MxCre*^{wt} mice and n=13 for *Gfi1b*$^{fl/fl}$*MxCre*^{tg}*NUP98/HOXD13*^{tg} mice).

C. The frequency of myeloid cells (****p<0.0001) in the BM of the mice described in Figure 3F (n=15 for *Gfi1b*$^{fl/fl}$*MxCre*^{wt} mice and n=13 for *Gfi1b*$^{fl/fl}$*MxCre*^{tg}*NUP98/HOXD13* mice).

D. Number of annexin-positive cells in the BM of the mice described in Figure 3F (n=15 for *Gfi1b*$^{fl/fl}$*MxCre*^{wt} mice and n=13 for *Gfi1b*$^{fl/fl}$*MxCre*^{tg}*NUP98/HOXD13* mice).

Supplementary Figure 4 Thivakaran et al.

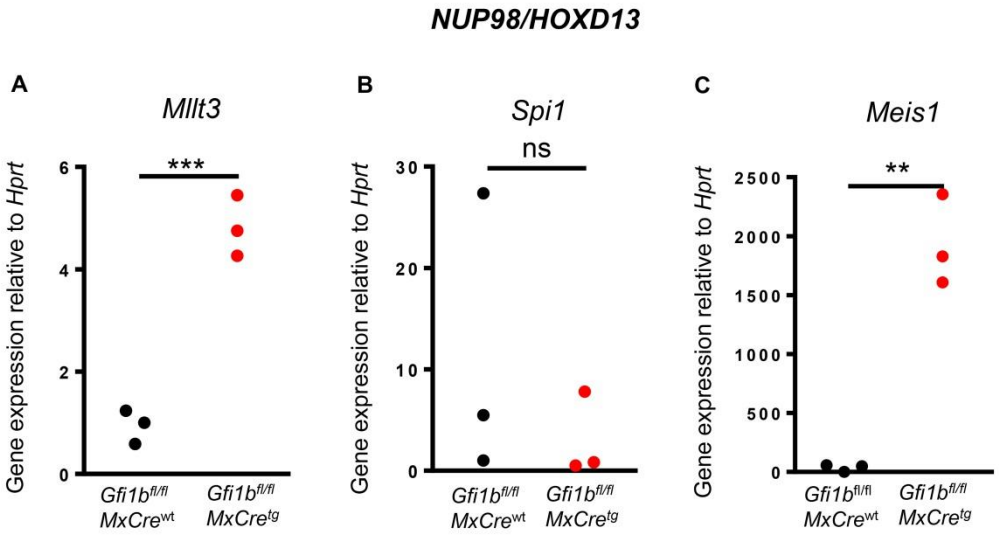

Supplementary Figure 4

A. *Mllt3* gene expression relative to *Hrpt* at the mRNA level in BM cells derived from *Gfi1b*$^{fl/fl}$ *x* *MxCre*^{tg}*NUP98/HOXD13*^{tg} mice (n=3) and *Gfi1b*$^{fl/fl}$ *x* *MxCre*^{wt}*NUP98/HOXD13*^{tg} mice (n=3) ***p=0.0006.

B. *Spi1* gene expression relative to *Hrpt* at the mRNA level in BM cells derived from *Gfi1b*$^{fl/fl}$ *x* *MxCre*^{tg}*NUP98/HOXD13*^{tg} mice (n=3) and *Gfi1b*$^{fl/fl}$ *x* *MxCre*^{wt}*NUP98/HOXD13*^{tg} mice (n=3).

C. *Meis1* gene expression relative to *Hrpt* at the mRNA level in BM cells derived from *Gfi1b*$^{fl/fl}$ *x* *MxCre*^{tg}*NUP98/HOXD13*^{tg} mice (n=3) and *Gfi1b*$^{fl/fl}$ *x* *MxCre*^{wt}*NUP98/HOXD13*^{tg} mice (n=3) **p=0.0010.

Supplementary Figure 5 Thivakaran et al.

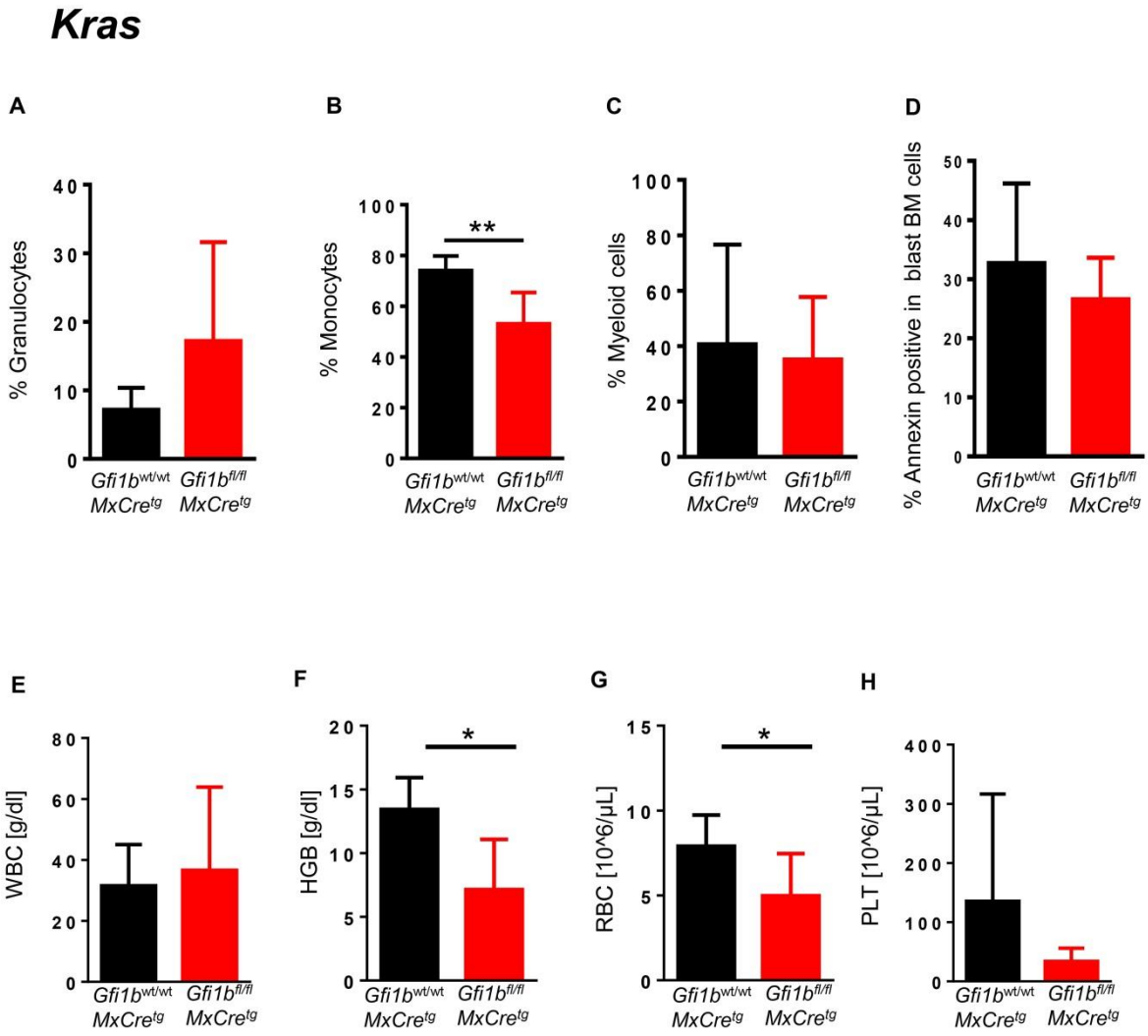

Supplementary Figure 5

A. The frequency of granulocytes (Mac-1^{hi}Gr-1^{hi}) (*p=0.0206) in the BM of the mice described in Figure 4B (n=4 for *Gfi1b$^{wt/wt}$MxCre^{tg} Kras* mice and n=10 for *Gfi1b$^{fl/fl}$MxCre^{tg} Kras* mice).

B. The frequency of monocytes (Mac-1^{hi}Gr-1^{int}) (**p=0.0084) in the BM of the mice described in Figure 4B (n=4 for *Gfi1b$^{wt/wt}$MxCre^{tg} Kras* mice and n=10 for *Gfi1b$^{fl/fl}$MxCre^{tg} Kras* mice).

C. The frequency of myeloid cells in the BM of the mice described in Figure 4B (n=4 for *Gfi1b$^{wt/wt}$MxCre^{tg} Kras* mice and n=10 for *Gfi1b$^{fl/fl}$MxCre^{tg} Kras* mice).

D. Number of annexin-positive cells in the BM of the mice described in Figure 4B (n=4 for *Gfi1b$^{wt/wt}$MxCre^{tg} Kras* mice and n=10 for *Gfi1b$^{fl/fl}$MxCre^{tg} Kras* mice).

E. Median values for white blood cell (WBC) count of *Gfi1b$^{wt/wt}$MxCre^{tg}* (n=4) and *Gfi1b$^{fl/fl}$MxCre^{tg}Kras$^{+/fl}$* (n=10) leukaemic mice.

F. Median values for haemoglobin (HGB) of *Gfi1b$^{wt/wt}$MxCre^{tg}* (n=4) and *Gfi1b$^{fl/fl}$MxCre^{tg}Kras$^{+/fl}$* (n=10) leukaemic mice, *p=0.0128.

G. Median values for red blood cell number (RBC) of *Gfi1b$^{wt/wt}$MxCre^{tg}* (n=4) and *Gfi1b$^{fl/fl}$MxCre^{tg}Kras$^{+/fl}$* (n=10) leukaemic mice, *p=0.0186.

H. Median values for platelet number (PLT) of *Gfi1b$^{wt/wt}$MxCre^{tg}* (n=4) and *Gfi1b$^{fl/fl}$MxCre^{tg}Kras$^{+/fl}$* (n=10) leukaemic mice.

Supplementary Figure 6 Thivakaran et al.

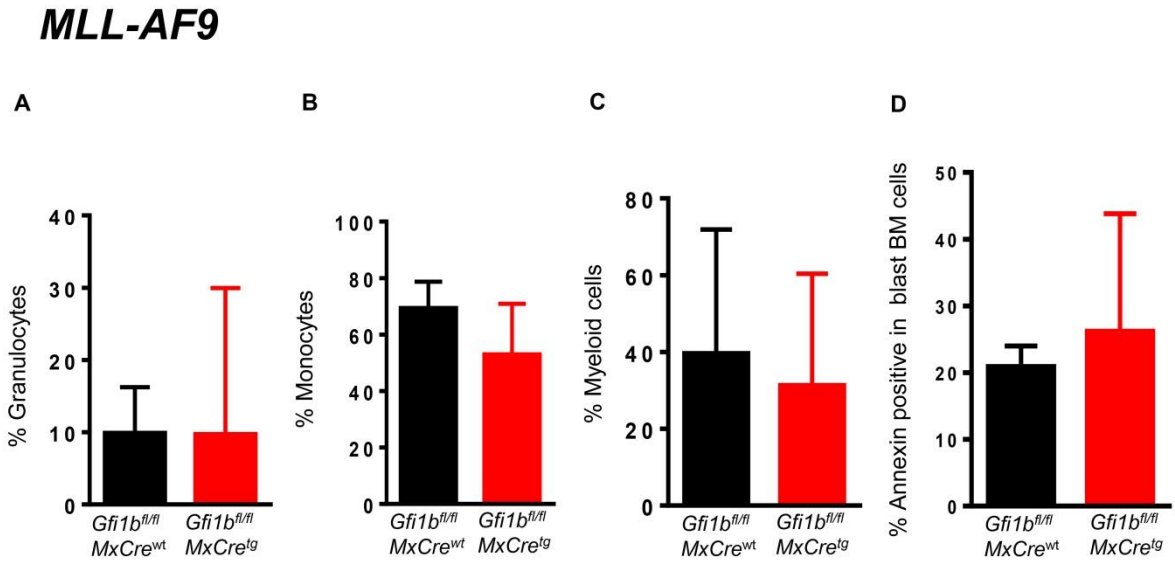

Supplementary Figure 6

A. The frequency of granulocytes (Mac-1^{hi}Gr-1^{hi}) in the BM of the mice described in Figure 4F (n=10 for *Gfi1b$^{fl/fl}$MxCre^{tg} MLL-AF9* mice and n=13 for *Gfi1b$^{fl/fl}$MxCre^{tg} MLL-AF9* mice).
B. The frequency of monocytes (Mac-1^{hi}Gr-1^{int}) in the BM of the mice described in Figure 4F (n=10 for *Gfi1b$^{fl/fl}$MxCre^{tg} MLL-AF9* mice and n=13 for *Gfi1b$^{fl/fl}$MxCre^{tg} MLL-AF9* mice).
C. The frequency of myeloid cells in the BM of the mice described in Figure 4F (n=10 for *Gfi1b$^{fl/fl}$MxCre^{tg} MLL-AF9* mice and n=13 for *Gfi1b$^{fl/fl}$MxCre^{tg} MLL-AF9* mice).
D. Number of annexin-positive cells in the BM of the mice described in Figure 4F (n=10 for *Gfi1b$^{fl/fl}$MxCre^{tg} MLL-AF9* mice and n=13 for *Gfi1b$^{fl/fl}$MxCre^{tg} MLL-AF9* mice).

Supplementary Figure 7 Thivakaran et al.

A

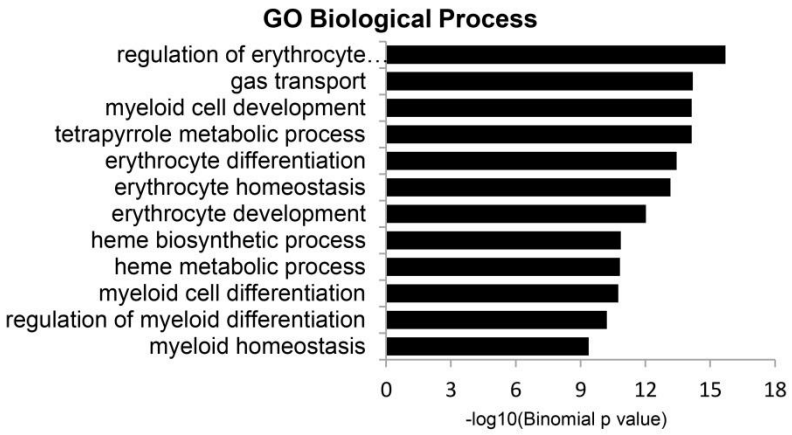

B

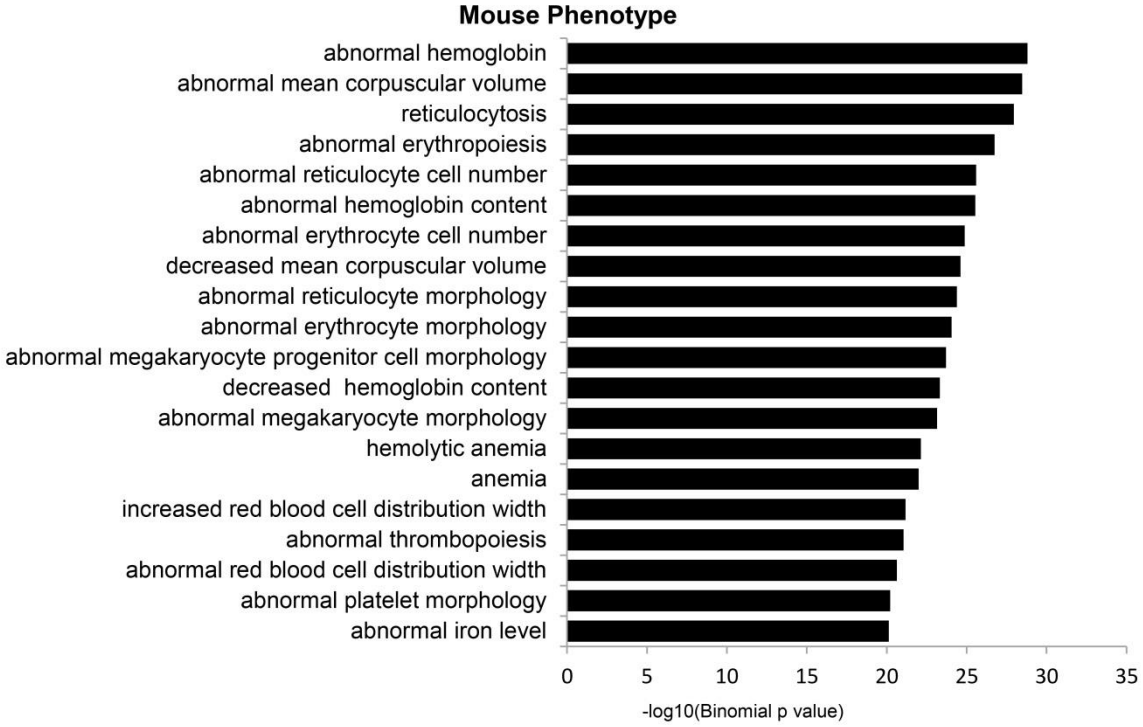

Supplementary Figure 7

A. GO Biological processes overrepresented among differentially acetylated genes in *Gfi1b*$^{fl/fl}$*MxCre*^{wt} and *Gfi1b*$^{fl/fl}$*MxCre*^{tg}*NUP98-HOXD13*^{tg} leukaemic mice, as determined using the DAVID software. P value was used to rank the enrichment.

B. Upon analysing the differentially acetylated genes and using the MSigDB Pathway approach, we found significant enrichment of a different phenotype. P value was used to rank the enrichment.

Supplementary Figure 8 Thivakaran et al.

A

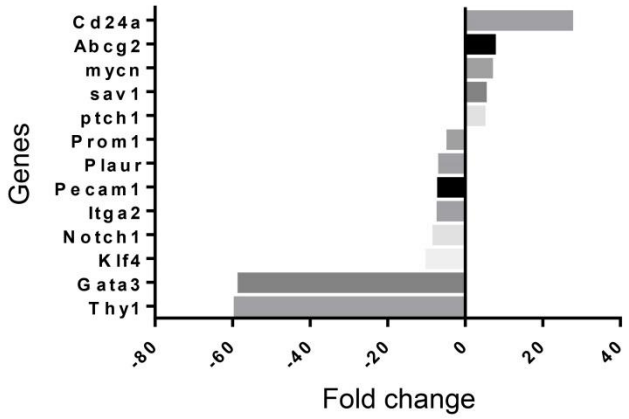

B

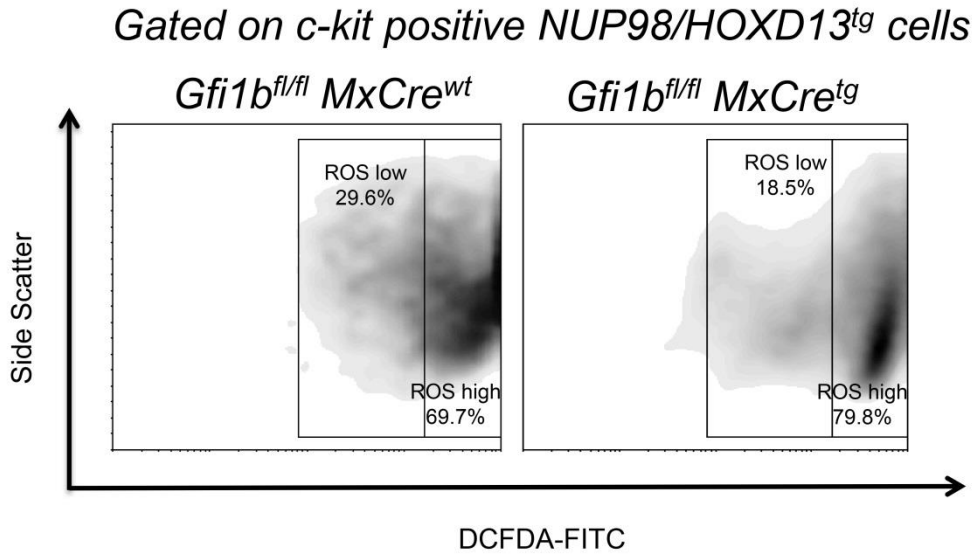

Supplementary Figure 8

A. Genes differentially regulated by more than 2-fold between *Gfi1b*-expressing and *Gfi1b*-deficient leukaemic mice in the gene expression arrays: *Abcg2, Gata3, Itga2, Thy1, Cd24a, Pecam1, Prom1, Plaur, Klf4, Mycn, Ptch1, Pecam1, Sav1,* and *Notch1*.
B. Representative FACS plot and gating strategy for define the ROS low and ROS high population in *Gfi1b*-deficient and *Gfi1b*-expressing leukaemic cells.

Supplementary Figure 9 Thivakaran et al.

A

Enriched TF-binding sites in promoters of regulated genes

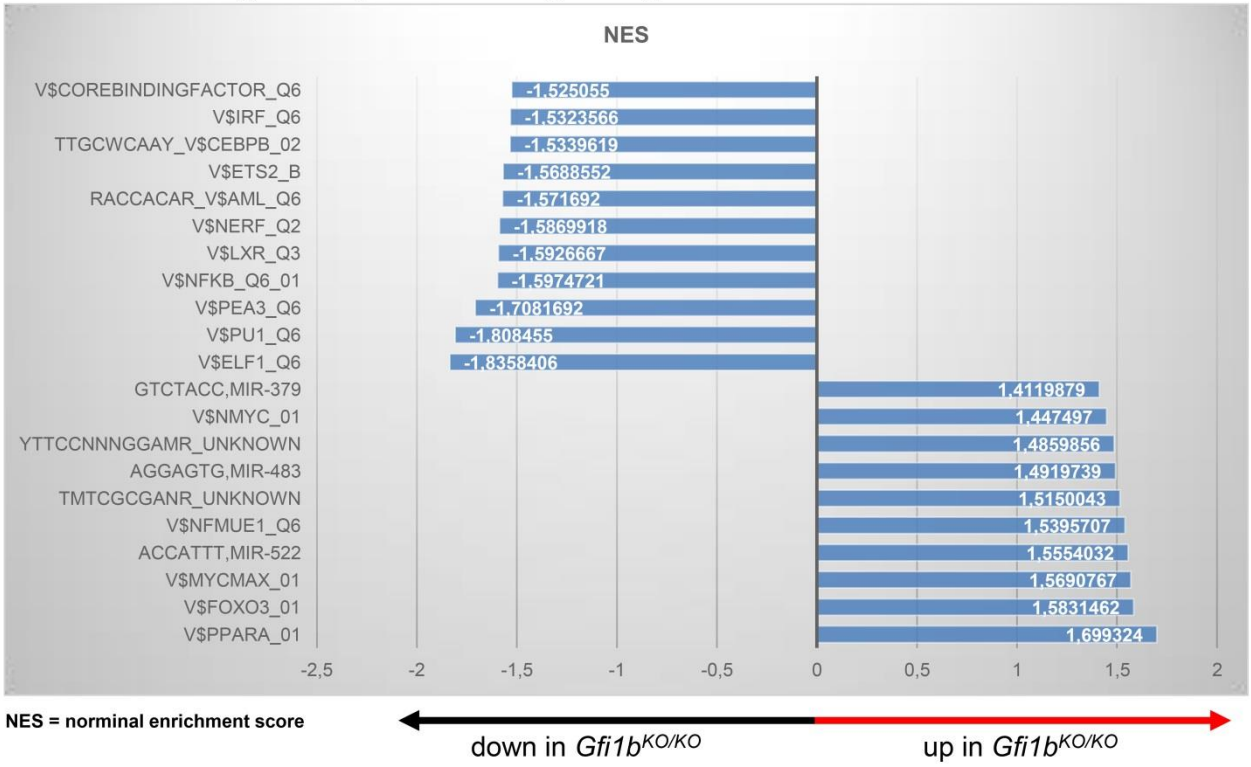

NES = norminal enrichment score

down in *Gfi1b*$^{KO/KO}$ up in *Gfi1b*$^{KO/KO}$

Supplementary Figure 9

A. Whole genome expression array analysis was performed with *Gfi1b* deficient BM leukemic cells and found an upregulation of genes regulated by FoXO3.

References

1. Emig D, Salomonis N, Baumbach J, Lengauer T, Conklin BR, Albrecht M. AltAnalyze and DomainGraph: analyzing and visualizing exon expression data. Nucleic Acids Res. 2010;38(Web Server issue):W755-762.
2. Parikh JR, Klinger B, Xia Y, Marto JA, Bluthgen N. Discovering causal signaling pathways through gene-expression patterns. Nucleic Acids Res. 2010;38(Web Server issue):W109-117.
3. Verhaak RG, Wouters BJ, Erpelinck CA, et al. Prediction of molecular subtypes in acute myeloid leukemia based on gene expression profiling. Haematologica. 2009;94(1):131-134.
4. Bluthgen N, Kielbasa SM, Herzel H. Inferring combinatorial regulation of transcription in silico. Nucleic Acids Res. 2005;33(1):272-279.
5. Khandanpour C, Sharif-Askari E, Vassen L, et al. Evidence that growth factor independence 1b regulates dormancy and peripheral blood mobilization of hematopoietic stem cells. Blood. 2010;116(24):5149-5161.
6. Subramanian A, Tamayo P, Mootha VK, et al. Gene set enrichment analysis: a knowledge-based approach for interpreting genome-wide expression profiles. Proceedings of the National Academy of Sciences of the United States of America. 2005;102(43):15545-15550.
7. Mootha VK, Lindgren CM, Eriksson KF, et al. PGC-1alpha-responsive genes involved in oxidative phosphorylation are coordinately downregulated in human diabetes. Nat Genet. 2003;34(3):267-273.